Relative intensity noise study in the injection-locked integrated electroabsorption modulator-lasers

Xiaomin Jin [a] , Bennet Yun Tarng [b], Shun-Lien Chuang [b]

[a] *Electrical Engineering Department, California Polytechnic State University, San Luis Obispo, CA 93407, USA*
[b] *Department of Electrical and Computer Engineering, University of Illinois at Urbana-Champaign, 1406 W. Green Street, Urbana, IL 61801, USA*

A B S T R A C T

We present a comprehensive analytical theoretical model for the relative intensity noise (RIN) spectrum of integrated semiconductor quantum-well (QW) lasers under injection-locking. We use a novel setup by employing an integrated electroabsorption modulator-laser (EML) to measure the RIN of the injection-locked distributed feedback (DFB) laser, where the modulator section is used as a photodetector. The EML has an anti-reflection coating on the laser side, so that an injection light from an external master laser can be coupled effectively into the laser section. This scheme simplifies the setup and reduces the alignment loss between discrete optical components. Experimental data indicates that the injection-locking technique can reduce the RIN noise floor and increase the relaxation frequency of the laser. We also compare the RIN spectra of the free-running laser with the injection-locked laser and show an increase of the relaxation frequency from 3.7 GHz (free-running) to 11.3 GHz (injection-locked). By fitting the experimental data using our model, we show very good agreement between our data and theory. Our model considers the optical confinement factor of photons and carriers for quantum-well structure lasers. We also improve the injection-locking RIN model by including the gain saturation from the master laser noise.

Keywords:
Optical injection
Injection-locking
Noise
Semiconductor laser

1. Introduction

An injection-locked laser system contains two semiconductor lasers. The light from a master laser is injected into the slave laser oscillating above threshold, and the injected radiation competes with the spontaneous emission of the slave laser being amplified. If the optical frequency of the injected light is close to the eigen-frequency of the unperturbed laser, the slave laser will adjust its frequency and coherence properties to that of the injected light. When a complete locked state is reached, all of the power of the slave laser is emitted at the optical frequency of the master laser. This phenomenon is known as injection-locking. Injection-locking technique is a promising candidate for high-bandwidth optical transmitters. For analog fiber optical communication system, this technique is an effective method to increase the laser relaxation oscillation frequency [1–7], improve laser bandwidth [1–7], reduce nonlinear distortions [8], suppress the frequency chirp and further reduce the laser system noise [9–13].

Relative intensity noise (RIN) is a very important property for semiconductor lasers which represents the laser's intrinsic resonance. For optical communication, low RIN floor is needed for the transmitter to achieve desirable signal-to-noise ratio (SNR). The intensity noise spectrum shows a peak near the relaxation frequency, which is an important parameter for the laser system and directly related to the bandwidth of the laser. Several theoretical simulations of noise characteristics have been reported [14–18] and have predicted relaxation frequency enhancement with injection-locking [14]. However, little experimental work on RIN spectra for injection-locked semiconductor lasers is available in the literature [9,13,14,19] to confirm the noise reduction of injection-locking system directly. This is due to high-fiber coupling loss, the optical signal is too weak to allow direct noise measurement by the current testing equipment. In Ref. [13], an EDFA followed by an optical filter were used to amplify the noise signal before sent into the lightwave analyzer for detection. This method actually will add EDFA noise into the injection-locked laser noise. In this paper, we report RIN experimental results and theoretical calculations of an injection-locked distributed feedback (DFB) laser using an integrated electroabsorption modulator-laser (EMLs) or integrated laser-modulators (ILMs), as they are also known. An electroabsorption modulator has commonly been developed monolithically with an integrated DFB laser to eliminate coupling loss at a joint [20–22]. This device has a higher reflection (HR) coating on the modulator side and an anti-reflection (AR) coating on the laser facet (Fig. 1). In our experiment, we use the reveres biased modulator as a photodetector and investigate the injection-locking noise phenomena of the DFB laser. With the modulators acting as

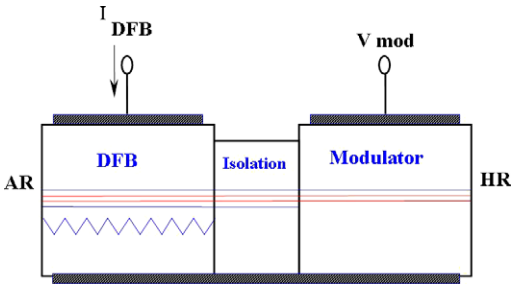

Fig. 1. The schematic diagram of an integrated electroabsorption modulator-laser. The laser facet is AR coated for optical output, and the modulator facet is HR coated. Between the DFB laser and the modulator is an electrical isolation section.

photodetectors, the number of connectors in our setup is reduced, the electrical signal can be directly measured, and a more accurate measurement is obtained. Also, the results for injection-locked EMLs give us an opportunity to confirm the theories of increased relaxation frequency in injection-locked DFB lasers directly. As a matter of fact, the external optical injection in integrated lasers is also a relatively uninvestigated field. Furthermore, this experimental and theoretical work also gives us insight on the integrated injection-locking detection system.

Our paper is organized as follows. In Section 2, we present a comprehensive analytical RIN theory of an injection-locked integrated semiconductor laser. In Section 3, the experimental data and theoretical calculation results of RIN of an injection-locked laser using an EML are discussed. Our conclusion is summarized in Section 4.

2. Theory of relative intensity noise of an injection-locked integrated semiconductor laser

A semiclassical analysis is used to analyze the RIN spectra of semiconductor lasers. To determine the laser RIN, we must obtain the total photon fluctuation in the cavity $\Delta S(t)$, the total carrier fluctuation $\Delta N(t)$, and instantaneous frequency deviation $\dot{\phi}(t)$ from their stationary values. Then we need to add appropriate Langevin noise in these equations, and find the power spectral density of the photon fluctuation. The rate equations for the slave laser field are based on Ref. [15], and we modify them according to the integrated semiconductor laser, add nonlinear gain saturation coefficients for both slave and master lasers, and insert the optical confinement factor of the QW laser structure:

$$\frac{dS(t)}{dt} = \left[\Gamma\left(G_0 + G_n\frac{\Delta N}{\Gamma V}\right)(1 - \varepsilon S(t) - \varepsilon_M S_M(t)) - \frac{1}{\tau_p}\right]S(t)$$

(Normal slave laser terms)

$$+2k\sqrt{S(t)S_M(t)}\cos(\phi(t) - \phi_M(t))$$

(Injection-locking terms by the injected laser)

$$+\frac{k_f}{\tau_{in}}S(t-\tau)\cos(\phi(t-\tau) - \omega_0\tau - \phi(t)) \quad (1)$$

(Optical feedback terms by the EML modulator)

$$\frac{d\phi(t)}{dt} = \frac{\alpha G_n}{2V}(1 - \varepsilon S(t) - \varepsilon_M S_M(t))\Delta N(t)$$

(Normal slave laser terms)

$$-(\omega_i - \omega_0) - k\sqrt{S(t)/S_M(t)}\sin(\phi(t) - \phi_M(t))$$

(Injection-locking terms by the injected laser)

$$+\frac{k_f}{\tau_{in}}\sqrt{\frac{S(t-\tau)}{S(t)}}\sin(\phi(t-\tau) - \omega_0\tau - \phi(t)) \quad (2)$$

(Optical feedback terms by the EML modulator)

$$\frac{dN(t)}{dt} = \frac{\Gamma VJ}{qd} - \frac{N(t)}{\tau_n}$$

$$-\Gamma\left(G_0 + G_n\frac{\Delta N}{\Gamma V}\right)[1 - \varepsilon S(t) - \varepsilon_M S_M(t)]S(t) \quad (3)$$

In the rate equations of photon density and phase of the slave laser, there are three catalogs of terms: (1) normal slave laser terms. We consider the additional gain saturation caused by the injected light; (2) additional terms because of injection-locking; and (3) optical feedback terms by the EML modulator section, according to the long and Kobayashi model [23–24]. For the optical feedback terms, k_f is the feedback parameter. The τ_{in} is the round trip time in the laser cavity, τ is the round trip time of the light in the modulator section. In our experiment, we reversed bias the modulator section and it acts as an absorption photodetector. It is known that when the biased electroabsorption section strongly absorbs light, the feedback is weak and does not affect the locking of the laser section. Therefore, in our final model, we neglect the optical feedback terms or set $k_f = 0$ to keep the model as simple as possible. The final equations are:

$$\frac{dS(t)}{dt} = \left[\Gamma\left(G_0 + G_n\frac{\Delta N}{\Gamma V}\right)(1 - \varepsilon S(t) - \varepsilon_M S_M(t)) - \frac{1}{\tau_p}\right]S(t) + 2k\sqrt{S(t)S_M(t)}\cos(\phi(t) - \phi_M(t)) \quad (4)$$

$$\frac{d\phi(t)}{dt} = \frac{\alpha G_n}{2V}(1 - \varepsilon S(t) - \varepsilon_M S_M(t))\Delta N(t) - (\omega_i - \omega_0) - k\sqrt{S(t)/S_M(t)}\sin(\phi(t) - \phi_M(t)) \quad (5)$$

$$\frac{dN(t)}{dt} = \frac{\Gamma VJ}{qd} - \frac{N(t)}{\tau_n} - \Gamma\left(G_0 + G_n\frac{\Delta N}{\Gamma V}\right)[1 - \varepsilon S(t) - \varepsilon_M S_M(t)]S(t) \quad (6)$$

where $S(t)$ and $S_M(t)$ are the total photon number of the slave laser and injected field, $\varphi(t)$ and $\varphi M(t)$ are the phase of the slave laser and injected field, ω_i and ω_0 are the injected field frequency and the slave laser resonance frequency, $k = c/(2n_gL)$ is coupling coefficient, c is the velocity of light in the vacuum, L and n_g are the length and the group index, respectively. τ_P is the photon lifetime, τ_n is the carrier lifetime, J is the current density, q is the unit charge, d is the active region thickness, $n(t)$ is the carrier density, α is the linewidth-enhancement factor, and Γ is the optical confinement factor of the QW laser structure [25]. In QW lasers, the carriers and photons occupy different volumes. The total number of photons in the slave laser is $S(t) = S_0 + \Delta S(t) = V|E(t)|^2$, while $E(t)$ is the optical field. The total number of carriers is $N(t) = \Gamma V\, n(t)$. V is the optical mode volume. The optical confinement factor is well-known to be important for separate confinement quantum-well structures; however, it is usually ignored in literature on injection-locking. G_0 is the cavity gain coefficient, and $G_n = dG/dn|_{n=n0}$ is the differential gain. The gain saturation is also included, where ε and ε_M are the nonlinear gain saturation coefficients corresponding to the slave laser signal and the injected signal. The nonlinear gain saturation coefficients have been used in earlier studies [26–28] on high-speed lasers where the gain of the slave laser light is suppressed due to the presence of the injected light. Ref. [26] employs two saturation terms because the injected light and the internal light have orthogonal polarizations. In our derivation, the injected light is slighted different from the slave light. They both have contribution to the slave laser gain saturation, which is also called the cross-gain saturation of laser amplifiers [29,30]. Therefore, in our simulation, we need to consider both effects and use $\varepsilon_M \sim \varepsilon$. This is an important phenomenon if we inject light in the laser gain region and it cannot be neglected. Actually, inclusion of Γ and ε_M is important to obtain consistent parameters for the gain and differential gain for quantum-well lasers. Finally,

the above equations show that the slave laser will be affected by the emission of the master laser. When a photon is spontaneously emitted in the master laser, it will cause deviations of the amplitudes and phases of the slave and master laser fields from their stationary values. Thus, we must consider the master laser noise characteristics when deriving the RIN of the slave laser.

Noise caused by spontaneous emission and carrier generation-recombination is included in the rate equations by adding the appropriate Langevin driving terms. For simplicity, we also assume that the Langevin noise sources of the slave laser are independent of the Langevin noises of the master laser. The two sets of noise sources are uncorrelated. Neglecting the higher order terms, the differential forms of the rate equations for the injection-locked laser system with Langevin noise terms ($F_{\Delta S}(t)$, $F_{\Delta\phi}(t)$, $F_{\Delta N}(t)$) and master laser noises ($\Delta S_M(t)$, $\Delta\phi_M(t)$) are

$$\Delta\dot{S}(t) = \left[\Gamma G_0(1-2\varepsilon S_0-\varepsilon_M S_{M0}) - \frac{1}{\tau_P} + k_c\right]\Delta S(t) + \frac{G_n S_0}{V}(1-\varepsilon S_0-\varepsilon_M S_{M0})\Delta N(t) - 2k_s S_0\Delta\phi(t) + (k_c S_0/S_{M0} - \Gamma G_0\varepsilon_M S_0)\Delta S_M(t) + 2k_s S_0\Delta\phi_M(t) + F_{\Delta S}(t) \quad (7)$$

$$\dot{\phi}(t) = \Delta\dot{\phi}(t) = k_s/(2S_0)\Delta S(t) - k_c\Delta\phi + \frac{\alpha G_n}{2V}(1-\varepsilon S_0-\varepsilon_M S_{M0})\Delta N(t) - k_s/(2S_{M0})\Delta S_M(t) + k_c\Delta\phi_M(t) + F_{\Delta\phi}(t) \quad (8)$$

$$\Delta\dot{N}(t) = -\Gamma G_0(1-2\varepsilon S_0-\varepsilon_M S_{M0})\Delta S(t) - \left[\frac{1}{\tau_n} + \frac{G_n S_0}{V}(1-\varepsilon S_0-\varepsilon_M S_{M0})\right]\Delta N(t) + \varepsilon_M\Gamma G_0 S_0\Delta S_M(t) + F_{\Delta N}(t) \quad (9)$$

where

$$k_c = k\sqrt{S_{M0}/S_0}\cos(\phi_0-\phi_{M0})$$

$$k_s = k\sqrt{S_{M0}/S_0}\sin(\phi_0-\phi_{M0})$$

We define $\Delta S(\omega)$, $\Delta\Phi(\omega)$, $\Delta N(\omega)$, $\Delta S_M(\omega)$, $\Delta\Phi_M(\omega)$, $F_{\Delta S}(\omega)$, $F_{\Delta\phi}(\omega)$, and $F_{\Delta N}(\omega)$ as the Fourier transforms of the truncated functions corresponding to $\Delta S(t)$, $\Delta\varphi(t)$, $\Delta N(t)$, $\Delta S_M(t)$, $\Delta\varphi_M(t)$, $F_{\Delta S}(t)$, $F_{\Delta\phi}(t)$, and $F_{\Delta N}(t)$. Using the Fourier transforms of Eqs. (7)–(9), and gain–loss relation derived from the steady-state solution of Eq. (4), $2k_c = 2k\sqrt{S_0 S_{M0}}\cos(\phi_0-\phi_{M0}) = -\Gamma G_0(1-\varepsilon S_0-\varepsilon_M S_{M0}) + \frac{1}{\tau_p}$, we obtain the following linear algebraic equations.

$$\begin{bmatrix} j\omega+a_{11} & a_{12} & a_{13} \\ a_{21} & j\omega+a_{22} & a_{23} \\ a_{31} & a_{32} & j\omega+a_{33} \end{bmatrix}\begin{bmatrix}\Delta S(\omega)\\ \Delta\Phi(\omega)\\ \Delta N(\omega)\end{bmatrix} = \begin{bmatrix} b_1(\omega)\\ b_2(\omega)\\ b_3(\omega)\end{bmatrix} \quad (10)$$

where

$$a_{11} = -k_c - \Gamma G_0(1-2\varepsilon S_0-\varepsilon_M S_{M0}) + \frac{1}{\tau_P}$$
$$a_{12} = 2k_s S_0$$
$$a_{13} = -G_n S_0(1-\varepsilon S_0-\varepsilon_M S_{M0})/V$$
$$a_{21} = k_s/(2S_0)$$
$$a_{22} = k_c$$
$$a_{23} = -\alpha G_n(1-\varepsilon S_0-\varepsilon_M S_{M0})/(2V)$$
$$a_{31} = \Gamma G_0(1-2\varepsilon S_0-\varepsilon_M S_{M0})$$
$$a_{32} = 0$$
$$a_{33} = \frac{1}{\tau_n} + G_n(1-\varepsilon S_0-\varepsilon_M S_{M0})S_0/V$$
$$b_1(\omega) = [k_c(S_0/S_{M0}) - \Gamma G_0\varepsilon_M S_0]\Delta S_M(\omega) + 2k_s S_0\Delta\Phi_M(\omega) + F_{\Delta S}(\omega)$$
$$b_2(\omega) = -k_s/(2S_{M0})\Delta S_M(\omega) + k_c\Delta\Phi_M(\omega) + F_{\Delta\phi}(\omega)$$
$$b_3(\omega) = F_{\Delta N}(\omega) + \varepsilon_M\Gamma G_0 S_0\Delta S_M(\omega) \quad (11)$$

The power spectral density of the slave laser photon can be obtained using the truncated function and Fourier analysis techniques [17]. Then, the RIN of the slave laser is obtained as

$$\frac{RIN}{\Delta f} = \frac{2}{S_0^2|Y(\omega)|^2}\left\{\frac{R_s G_n^2 S_0^2}{V^2}(1-2\varepsilon S_0-2\varepsilon_M S_{M0})[\omega^2+\gamma_k^2] + (\omega^2+k_c^2)(\omega^2+\gamma_e^2)L_1(\omega) + 4k_s^2 S_0^2(\omega^2+\gamma_e^2)L_2(\omega) - 4k_s S_0(\omega^2+\gamma_e^2)\mathrm{Re}[(i\omega+k_c)L_3(\omega)] + \frac{2G_n S_0}{V}(1-\varepsilon S_0 - \varepsilon_M S_{M0})\mathrm{Re}[(j\omega+k_c)(j\omega+\gamma_e)(-j\omega+\gamma_k)L_4(\omega)] + \frac{4k_s G_n S_0^2}{V}(1-\varepsilon S_0-\varepsilon_M S_{M0}) \times \mathrm{Re}[(j\omega-\gamma_k)(j\omega+\gamma_e)L_5(\omega)]\right\} \quad (12)$$

where Re[...] stands for "the real part of [...]", $\gamma_e = \frac{1}{\tau_n} + G_n(1-\varepsilon S_0-\varepsilon_M S_{M0})S_0/V$ which is determined by the carrier lifetime, the slave photon number, and the cavity gain, $\gamma_k = k_c - k_s\alpha$ which is related to the phase difference and detuning between the slave and master lasers, and

$$L_1(\omega) = \left(k_c\frac{S_0}{S_{M0}} - \Gamma G_0\varepsilon_M S_0\right)^2 P_{\Delta S_M}(\omega) + 4k_s^2 S_0^2 P_{\Delta\Phi_M}(\omega) + R_s(2S_0+1) + 4k_s S_0^2\left(\frac{k_c}{S_{M0}} - \Gamma G_0\varepsilon_M\right)\mathrm{Re}[P_{\Delta S_M\Delta\Phi_M}(\omega)] \quad (13)$$

$$L_2(\omega) = \frac{R_s}{2S_0} + \frac{k_s^2}{4S_{M0}^2}P_{\Delta S_M}(\omega) + k_c^2 P_{\Delta\Phi_M}(\omega) - \frac{k_c k_s}{S_{M0}}\mathrm{Re}[P_{\Delta S_M\Delta\Phi_M}(\omega)] \quad (14)$$

$$L_3(\omega) = \frac{1}{2S_{M0}}(\Gamma G_0\varepsilon_M S_0 k_s - \frac{k_c k_s S_0}{S_{M0}})P_{\Delta S_M}(\omega) + 2k_c k_s S_0 P_{\Delta\Phi_M}(\omega) - k_s^2\frac{S_0}{S_{M0}}P_{\Delta\Phi_M\Delta S_M}(\omega) + (k_c^2\frac{S_0}{S_{M0}} - k_c\Gamma G_0\varepsilon_M S_0)P_{\Delta S_M\Delta\Phi_M}(\omega) \quad (15)$$

$$L_4(\omega) = -R_s + \frac{k_c\Gamma G_0\varepsilon_M S_0^2}{S_{M0}}P_{\Delta S_M}(\omega) \quad (16)$$

$$L_5(\omega) = -\frac{k_s\Gamma G_0\varepsilon_M S_0}{2S_{M0}}P_{\Delta S_M}(\omega) \quad (17)$$

In the equations above, $P_{\Delta S_M}(\omega)$, $P_{\Delta S_M\Delta\Phi_M}(\omega)$, $P_{\Delta\Phi_M}(\omega)$, and $P_{\Delta\Phi_M\Delta S_M}(\omega)$ are the power spectra of the free-running master laser, which can be obtained by setting $S_M(t) = 0$ in Eqs. (4)–(6). $|Y(\omega)|^2$ is the denominator of the RIN of the slave laser

$$Y(\omega) = j\omega(\omega_r^2-\omega^2) - \omega^2\gamma + A \quad (18)$$

where

$$A = k^2\gamma_e\frac{S_{M0}}{S_0} + k_c\gamma_e\Gamma G_0\varepsilon S_0 + \frac{\gamma_k G_n S_0\Gamma G_0}{V}(1-3\varepsilon S_0-2\varepsilon_M S_{M0}) \quad (19)$$

The relaxation frequency of the slave laser is

$$\omega_r^2 = \frac{1}{\tau_n}\Gamma G_0(2\varepsilon S_0-1) + \frac{1}{\tau_P V}G_0 S_0(1-\varepsilon S_0) + \frac{1}{\tau_p\tau_n} + k^2\frac{S_{M0}}{S_0} + \Gamma G_0\left[\frac{\varepsilon_M S_{M0}}{\tau_n} + \frac{1}{2}\varepsilon S_0\left(\frac{1}{\tau_P} - \Gamma G_0\right)\right] - \frac{G_0\varepsilon_M S_0 S_{M0}}{\tau_P V}$$
$$= \omega_{r\,free}^2 + k^2\frac{S_{M0}}{S_0} + \Gamma G_0\left[\frac{\varepsilon_M S_{M0}}{\tau_n} + \frac{1}{2}\varepsilon S_0\left(\frac{1}{\tau_P} - \Gamma G_0\right)\right] - \frac{G_0\varepsilon_M S_0 S_{M0}}{\tau_P V} \quad (20)$$

The damping factor of the injection-locked laser is

$$\gamma = \Gamma G_0(2\varepsilon S_0 - 1) + \frac{G_n S_0}{V}(1 - \varepsilon S_0) + \frac{1}{\tau_n} + \frac{1}{\tau_P} + \varepsilon_M S_{M0}\left(\Gamma G_0 - \frac{G_n S_0}{V}\right)\left(= \gamma_{free} + \varepsilon_M S_{M0}\left(\Gamma G_0 - \frac{G_n S_0}{V}\right)\right(\quad (21)$$

where terms of a higher order, $\varepsilon^2 S_0^2$ or $\varepsilon S_0 \varepsilon_M S_{M0}$, have been neglected. ω_{rfree} and γ_{free} are the relaxation frequency and the damping factor of the free-running laser, respectively. The nonlinear gain saturation term due to the master laser, which represents the gain change caused by the master laser injection, modifies the damping factor of the laser system.

For a free-running laser, there are no injected-photon $S_M(t) = 0$ or $S_{M0} = 0$ and $\frac{1}{\tau_n} \approx \Gamma G_0$. Thus, $k_c = k_s = \gamma_k = 0$. We input those values into Eqs. (4)–(6) and obtain the RIN, the relaxation frequency, and the damping factor of a free-running laser.

$$\frac{\mathrm{RIN}}{\Delta f} = \frac{2R_s}{S_0^2}\frac{\left[\frac{G_n S_0(1-\varepsilon S_0)}{V}\left(\frac{G_n(1-\varepsilon S_0)S_0}{V} - 2\gamma_{e\ free}\right) + (2S_0+1)(\gamma_{e\ free}^2 + \omega^2)\right]\left(}{\left[\left(\omega_{r\ free}^2 - \omega^2\right)^2 + \gamma_{free}^2\omega^2\right]\left(} \quad (22)$$

where $\gamma_{e\ free} = \frac{1}{\tau_n} + G_n S_0(1 - \varepsilon S_0)/V$. The relaxation frequency of the free-running laser is

$$\omega_{r\ free}^2 = \frac{1}{\tau_n}\Gamma G_0(2\varepsilon S_0 - 1) + \frac{1}{\tau_P V} G_0 S_0(1 - \varepsilon S_0) + \frac{1}{\tau_P \tau_n} \quad (23)$$

The damping factor of the free-running laser is

$$\gamma_{free} = \Gamma G_0(2\varepsilon S_0 - 1) + \frac{G_n S_0}{V}(1 - \varepsilon S_0) + \frac{1}{\tau_n} + \frac{1}{\tau_P} \quad (24)$$

Compared with a free-running laser, the injection-locked laser is a third-order system instead of a second-order system (free-running), as shown by Eqs. (18) and (21). The injected-photon modifies the slave laser cavity properties, such as cavity gain decrease, relaxation frequency increase, and damping factor variation.

3. Study injection-locking using integrated electroabsorption modulator-lasers

3.1. Integrated electroabsorption modulator-lasers and their static characteristics

The structure of the integrated electroabsorption modulator-laser used is shown in Fig. 1. The device has three sections, which are a distributed feedback (DFB) laser section, an electroabsorption modulator section, and an electrode isolation section. The length of the DFB section is 300 μm, the isolation region is 83 μm, and the modulator section is 250 μm. The section between the laser and the modulator provides electrical isolation in the design.

The light–current (*L*–*I*) curves for this integrated electroabsorption modulator-laser were measured as function of modulator voltage and they are shown in Fig. 2a. The power output is always measured from the AR-coated facet. The optical spectra of the EML at 30 mA current bias and different modulator voltage biases are shown in Fig. 2b. The wavelength versus the current bias of the DFB laser and voltage bias of the modulator is summarized in Fig. 2c. The optical output power from the laser is not influenced much by the modulator bias. There is also no mode-hopping for this device when changing the voltage bias. When the modulator is reverse-biased, the absorption in the modulator section increases due to Franz–Keldysh or quantum-confined Stark effects.

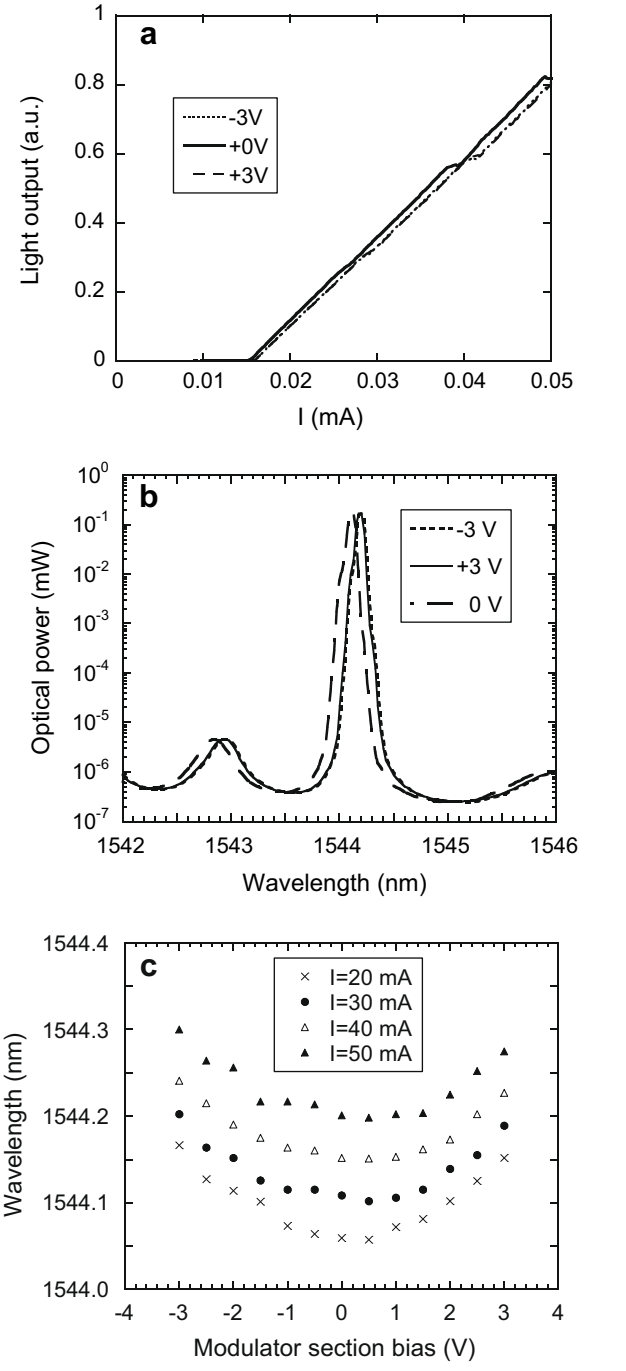

Fig. 2. (a) The light output versus the DFB laser bias current, (b) optical spectra at three modulator bias, and (c) the DFB laser wavelength at four bias current (*I* = 20, 30, 40, and 50 mA) as a function of the modulator bias voltage for the integrated electroabsorption modulator-laser.

When the modulator is forward-biased, the gain in the modulator section increases due to the carrier injection [32]. If looking into the modulator section from the isolation section, the modulator section can be viewed as an effective reflection coefficient and phase for the optical field at that boundary, which can perturb the longitudinal photon density profile of the laser cavity and modify the cavity properties. For our device, the waveguide in the laser section is straight, and the constant pitch of the laser already defines a specific Bragg wavelength and lasing wavelength. Thus the influence of the modulator section on the DFB laser wave-

length is mainly a small wavelength shift and not mode-hopping [32].

3.2. RIN of injection-locked integrated electroabsorption modulator-lasers

In this section, we present the experimental results of external injections in an integrated electroabsorption modulator-laser, using the modulator section of the EML as a photodetector. This experiment utilizes the advantage of photonic integrated circuit (PIC) technique to eliminate the disadvantages of using a more complicated setup with a separate photodetector as presented in [9]. The experimental setup is shown in Fig. 3. The injection signal from a single-mode DFB master laser passes through an erbium-doped fiber optical amplifier (EDFA). A tunable 3-nm bandwidth optical filter is used to remove excess signals on the side modes. The injection level is monitored by an optical power meter before it is injected into the EML where the laser section acts as a slave laser. The optical signal is converted to an electrical signal using the modulator photocurrent, amplified by an 18-dB gain microwave amplifier, and measured by the electrical spectrum analyzer to obtain the RIN spectra of the locked laser section output. A T-Bias is used to apply dc voltage onto the modulator section. In our setup, the method of external injection is similar to typical injection-locking with discrete semiconductor lasers. The difference arises in the method of photo-detection of the slave laser output for electrical analysis. In this case, the photodetection occurs in the modulator section instead of using another high-speed photodetector.

The influence of the modulator bias on the DFB laser should be very small so that any bias change or fluctuation in the modulator will not change the detuning between the master laser and the DFB laser on the EMLs, thus varying the injection condition and causing the laser system to become unlocked. When we bias the DFB laser of the EML at 30 mA, the wavelength difference between 0 V and −1 V modulator voltage is only 0.006 nm or 0.75 GHz (see Fig. 2c). This small difference will not switch the laser from the locked to the unlocked state, which ensures that the photocurrent generation is relatively independent at this voltage range. But the wavelength difference between 0 V and −2 V is 0.04 nm (5 GHz). This wavelength change cannot be neglected. Therefore, in our experiment we only bias our modulator at 0 V and −1 V. Fig. 2c also shows that 0 V bias occurs at the zero slope or near zero derivative of the wavelength–voltage curve, which is an ideal bias point to measure the photocurrent spectra.

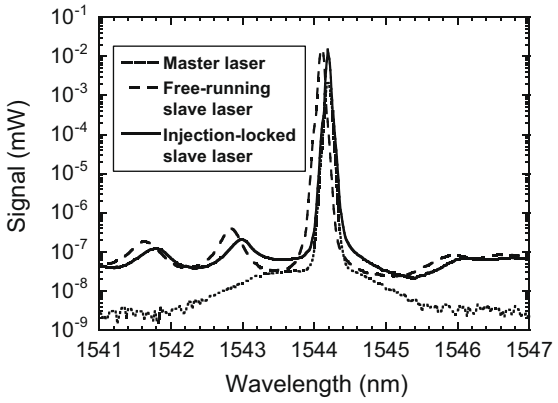

Fig. 4. Optical spectra of the external master (injection) laser, the integrated EML without injection (free-running slave laser), and the injection-locked EML under external injection light in the injection-locking experiment. The DFB laser of the EML (slave laser) is biased at 30 mA, and the modulator is biased at 0 V.

The optical spectra of the injection-locking experiment using the EML are shown in Fig. 4. With the master laser turned off and the DFB slave laser of the EML biased above threshold, there is no external injection, and the slave laser is free-running. During the experiment, the modulator is biased at 0 V. The free-running slave laser is lasing at 1544.1 nm (30 mA bias) with a side-mode suppression ratio (SMSR) of 44 dB. The master laser lases at 1544.2 nm with 50 dB SMSR. The detuning between the two lasers is 12.6 GHz. The injection-locked laser has the same lasing wavelength as the master laser and 50 dB SMSR. Thus, the injection light has caused the slave laser to lase at the master laser wavelength, resulting in an injection-locked condition. The RIN data of the injection-locked DFB laser is shown in Fig. 5a. From these measurements, we observe that the RIN peak shifts in frequency and amplitude varies as a function of the injection intensity. The data are limited by the noise floor of the electrical spectrum analyzer, which are around −130 dB/Hz for low frequency range (between 21 MHz and 6.26 GHz) and −126 dB/Hz for high frequency range (between 6.26 GHz and 12 GHz). We cannot resolve the signal below this level. But we can still observe the reduction of the RIN floor level under external injection. The spectra with higher injection power under injection-locking condition are below the noise limit of the spectrum analyzer and lower than the free-running slave laser (−126 dB/Hz) at low frequency range. The relaxation frequency peak is around 3.7 GHz for the free-running laser. The

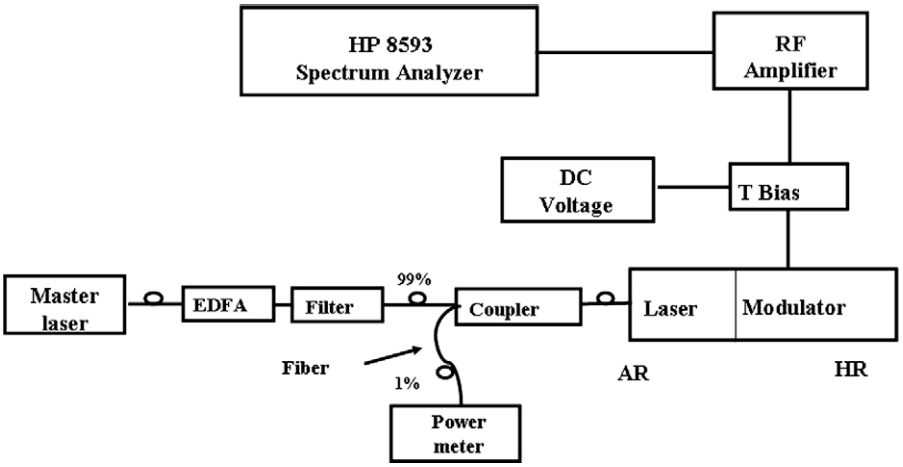

Fig. 3. Experimental setup of RIN measurement of the injecting-locked DFB laser using the integrated electroabsorption modulator-laser. The pump light from the master laser is injected into the AR facet of the integrated EML and the modulator is used as a photodetector.

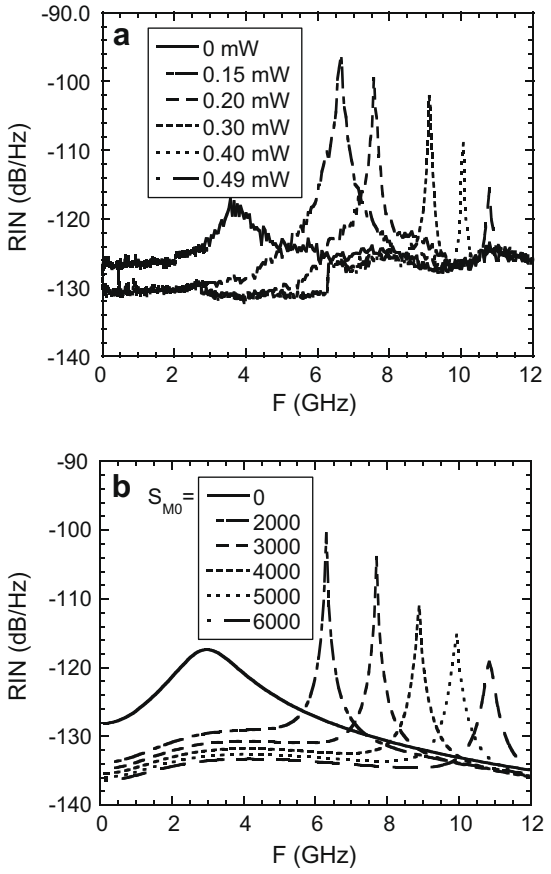

Fig. 5. (a) Experimental data and (b) theoretical calculation of RIN spectra of an injection-locked DFB laser system.

Table 1
The laser modeling parameters.

Parameter	Symbols	Value
Cavity length	L	300 μm
Active volume	V	3.89×10^{-10} cm^3
Effective index of refraction	n_g	3.33
Group velocity	v_g	9.0×10^9 cm s^{-1}
Mirror loss	αm	42.15 cm^{-1}
Intrinsic loss	αi	23 cm^{-1}
Optical confinement factor	Γ	0.15
Linewidth-enhancement factor	α	1.8
Photon lifetime	τ_p	8.5 ps
Carrier lifetime	τ_n	0.13 ns
Differential gain	$g'_l = g'_u$	3.6×10^{-16} cm^2
Nonlinear gain saturation coefficient	$\varepsilon_M \sim \varepsilon$	2.32×10^{-17} cm^3

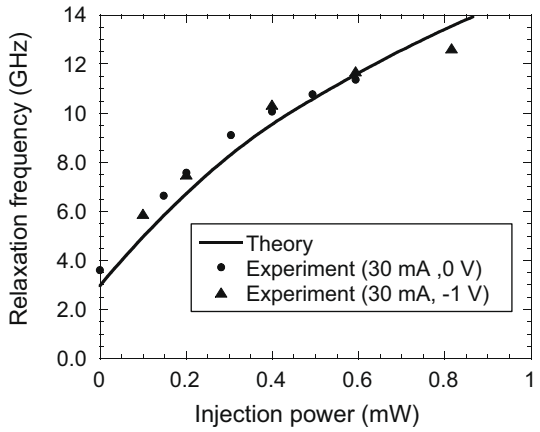

Fig. 6. The relaxation frequency versus different injection power of the injection-locked laser system. The injection power is monitored by an optical power meter before it is injected into the EML in the experiment. In the theory, a linear relation $P_{in}(mW) = 0.031\ S_{M0}$ is used to convert the calculated injected-photon number into the injection power.

maximum observed relaxation frequency is 11.3 GHz, which is three times the free-running value. As the injection intensity is increased further, the RIN peak attenuates and drops below the noise level. Our theoretical results are shown in Fig. 5b, which agree with our experimental data. The theory clearly shows higher injection level results in a lower noise floor and a larger relaxation frequency. The values of the physical parameters are $\Gamma = 0.15$, $\tau_p = 8.5$ ps, $V = 3.89 \times 10^{-10}$ cm^3, $G_0 = 8.7 \times 10^{11}$ s^{-1}, $G_n = 2.3 \times 10^{-5}$ cm^3 s^{-1}, $\tau_n = 0.13$ ns, $\alpha = 1.8$, $k = c/(2n_gL) = 1.5 \times 10^{11}$ s^{-1}, $L = 300$ μm, $R_s = 2 \times 10^{12}$ s^{-1}, and $n_g = 3.33$. The other important laser model parameters are listed in the Table 1. In our calculation, some of the parameters such as the effective index of refraction, intrinsic loss, and the initial value of the differential gain are obtained from independent measurements using the methods proposed in Ref. [25]. The linewidth-enhancement factor was obtained by measuring the injection-locking range [34]. The final value of the differential gain and gain saturation coefficients are fitting parameters. To simplify the calculation, because the wavelength of the injected signal and the slave signal are very close, we use $\varepsilon_M \sim \varepsilon$. The relaxation frequency versus injection power is plotted in Fig. 6. The symbols are experimental data, and the line represents theoretical results. We use a linear relation $P_{in}(mW) = 0.031 S_{M0}$ to convert the calculated injected-photon number into the injection power to compare with the experimental data. We also measure the RIN at -1 V modulator bias, and the results overlap with our 0 V data as expected. This confirms that the modulator bias has minimal influence on the DFB laser section. The modulator acts as a photodetector in our experiment to obtain the RIN of the injection-locked laser section, which is much simpler and easier than using discrete devices [9].

Our results also show theoretically that the coherent addition of the injected optical field to the slave laser optical field in the slave laser cavity is the main reason for the improvement of relaxation frequency. Without any injected signal $S_M(t) = 0$, the rate equations of the slave laser amplitude and phase are uncoupled (see Eqs. (4) and (5)). Also the phase term is not necessary to solve for the total photon spectrum. In an injection-locked laser system, the injected-photon term connects the amplitude and phase of the slave laser. The additional terms in the relaxation frequency of the injection-locked laser system come from the phase-amplitude coupling. Our theory also shows that the enhancement of the relaxation frequency can be attributed to the intensity of the injected field and the gain change (caused by nonlinear gain saturation terms). Generally, any change in the injection power or the gain will alter the relaxation resonance frequency [31]. Furthermore, an important effect of external optical injection in the stable locking regime is reduction of the cavity gain due to a reduction in carrier density, which shifts the optical resonance frequency and eventually modifies the relaxation frequency [7,31,33]. Note that our model also includes the optical confinement factor of the separate confinement heterostructure QW laser and gain saturation from the injected signal compared to the other RIN models, which are important to obtain a reasonable value of differential gain.

Finally, our data clearly show that as long as we keep the modulator section slightly revised biased, the modulator section of EML can be acted as an independent detector, which has little feedback to change the injection-locking in the laser section. This is the first

step to study an integrated injection-locking detection system. And our data approves it is achievable. Since the EML used is an already-to-use and easy-to-obtain device, it is our first choice for the experimental study of injection-locking in the integration device. In the future, it is very meaningful to solve Eqs (1)–(3) and obtain complete injection-locking model in the integrate devices to reveal the feedback effects.

4. Conclusions

In this paper, we have shown experimentally and theoretically that the injection-locking technique can improve the relaxation frequency of the slave laser, as well as lower the RIN floor level. In our experiment, we use an integrated electroabsorption modulator-laser, which simplifies the experimental setup and reduce loss in data acquisition. The static properties of the used EML are described, including its physical structure and operation. The experimental results of the external injection in EMLs are shown, emphasizing a novel method of obtaining the electrical spectra of the output light by directly measuring the output photocurrent of the EML modulator section. This differs from all previous external injection experiments, which use a separate photodetector to produce the modulated photocurrent. In summary, besides present a comprehensive analytical theoretical model for the relative intensity noise (RIN) spectrum of integrated semiconductor quantum-well (QW) lasers under injection-locking, we also explore the possibility of the injection-locking photonic integrated circuit (PIC) technique.

Acknowledgments

We thank Cal Poly C3RP 2005 and 2007 grant (The Department of the Navy, Office of Naval Research, under Award # ONR N00014-05-1-0855 and ONR N00014-07-1-1152) and Agilent Global Research Funding 2006 and 2007 (Contract # 07-040 and 08-146) for the support of this research.

References

[1] Lidoyne O, Gallion PB, Erasme D. IEEE J Quant Electron 1991;27:344.
[2] Chen HF, Liu JM, Simpson TB. Opt Commun 2000;173:349.
[3] Simpson TB, Liu JM. IEEE Photon Technol Lett 1997;9:1322.
[4] Wang J, Haldar MK, Lin L, Mendis FVC. IEEE Photon Technol Lett 1996;8:34.
[5] Meng XJ, Chau T, Wu MC. Electron Lett 1998;34:2031.
[6] Haldar MK, Coetzee JC, Gan KB. IEEE J Quant Electron 2005;41:280.
[7] Jin X, Chuang SL. Solid-State Electron 2006;50:1141.
[8] Lang R. IEEE J Quant Electron 1982;QE-18:976.
[9] Jin X, Chuang SL. Appl Phys Lett 2000;77:1250.
[10] Yabre G. J Lightwave Technol 1996;14:2367.
[11] Harb CC, Ralph TC, Huntington EH, Fretiage I, McClelland DE, Bachor H. Phys Rev A 1996;54:4370.
[12] Huntington EH, Buchler BC, Harb CC, Ralph TC, McClelland DE, Bachor H. Opt Commun 1998;145:359.
[13] Chrostowski L, Zhao X, Chang-Hasnain CJ. IEEE T Microw Theory 2006;54(2):788.
[14] Simpson TB, Liu JM, Gavrielides. IEEE Photon Technol Lett 1995;7:709.
[15] Espana-Boquera MC, Puerta-Notario A. Electron Lett 1996;32:818.
[16] Yabre G, Wardt HD, Van den Boom HPA, Khoe GD. IEEE J Quant Electron 2000;36:385.
[17] Spano P, Piazzolis S, Tamburrini M. IEEE J Quant Electron 1986;QE-22:427.
[18] Schunk N, Petermann K. IEEE J Quant Electron 1986;QE-22:642.
[19] Hong Y, Shore KA. IEEE J Quant Electron 1999;35:1713.
[20] Tanbun-Ek T, Adams L, Nykolak G, Bethea C, People R, Sergent A, Wisk P, Sciortino P, Chu S, Fullowan T, Tsang WT. IEEE J Sel Top Quant Electron 1997;3:960.
[21] Bigan E, Ougazzaden A, Huet F, Carre M, Carenco A, Mircea A. Electron Lett 1991;27:1607.
[22] Wakita K, Kotaka I, Mitomi O, Asai H, Kawamura Y. IEEE Photon Technol Lett 1991;3:138.
[23] Lang R, Kobyashi K. IEEE J Quant Electron 1980;QE-16:347.
[24] Masoller C. IEEE J Quant Electron 1997;33:796.
[25] Minch J, Park SH, Keating T, Chuang SL. IEEE J Quant Electron 1999;35:1526.
[26] Eom J, Su CB. Appl Phys Lett 1989;54:1734.
[27] Lange CH, Su CB. Appl Phys Lett 1989;55:1704.
[28] Vassilovski D, Wu TC, Kan S, Lau KY, Zah CE. IEEE Photon Technol Lett 1995;7:706.
[29] Jin X, Keating T, Chuang SL. IEEE J Quant Electron 2000;36:1485.
[30] Qasaimeh O. J Lightwave Technol 2008;26:449.
[31] Lin L. IEEE J Quant Electron 1994;30:1701.
[32] Hsu A, Chuang SL, Fang W, Adams L, Nykolak G, Tanbun-Ek T. IEEE J Quant Electron 1999;35:961.
[33] Simpson TB, Liu JM, Gavrielides A. IEEE J Quant Electron 1999;35:961.
[34] Liu G, Jin X, Chuang SL. IEEE Photon Technol Lett 2001;13:430.